38th ELECTRONICS COMPONENTS CONFERENCE 1988

1988 PROCEEDINGS

38th ELECTRONIC COMPONENTS CONFERENCE

May 9–11, 1988

The Biltmore Hotel • Los Angeles, California

The Electronic Components Conference (ECC) is recognized as the premier international forum for presenting the latest developments associated with the design, fabrication, and use of electronic materials, devices, components, and systems. In the previous 37 conferences, the ECC has demonstrated its ability to produce provocative presentations and discussions concerning the development, manufacturing technology, and reliability of a broad spectrum of electronic components and hybrids.

This conference is sponsored jointly by the Components, Hybrids, and Manufacturing Technology Society of the IEEE and the Electronic Industries Association.

Future dates ECC conferences are:

1989 • May 22–24
The Westin Hotel Houston, Texas

1990 • May 20–23
The Bally Hotel Las Vegas, Nevada

1991 • May 11–16
The Westin Peachtree Plaza Atlanta, Georgia

1992 • San Diego, California

Library of Congress Number 78-647174

Awards

Best of Conference Paper

The Electronics Components Conference each year is proud to select the "Best of Conference" paper from the preceding ECC.

The winning authors receive from the IEEE/CHMT Society a certificate and a check for $500 as well as a plaque commemorating their achievement. Where multiple authors are involved, each receives a certificate and plaque, and they share the prize money.

Mr. **C. J. Bartlett,** Mr. **J. M. Segelken,** and Mr. **N. A. Teneketges,** AT&T Bell Laboratories, are the recipients of this year's top award for their paper, "Multi-Chip Packaging Design for VLSI-Based Systems."

C. J. Bartlett

J. M. Segelken

N. A. Teneketges

Outstanding Papers

This year, two "Outstanding Papers" have been also selected from last year's conference. The papers chosen are:

Mr. **J. C. Bolger,** Amicon Corporation
"Stress-Related Corrosion Failure of Plastic Encapsulated IC's During PTH Reliability Tests"

K. Seshan, S. N. S. Reddy, and **S. K. Ray,** IBM Corporation "Adhesion of Thin Metal Films to Polyimide"

Guest Speakers

Monday, May 9

ECC Luncheon Speaker
Dr. **Robert A. Laudise,** Director of the Materials Chemistry Research Laboratory, AT&T Bell Laboratories
"Status of Superconductive Materials and Opportunities for Applications"

Dr. Laudise gives a brief review of the history of oxide superconductors that led up to the discovery of high-Tc superconductors. The discovery and the crystal chemistry of the potassium-nickel-fluoride and perovskite structures are reviewed. Progress on the preparation of ceramics, single crystals, thin films, wire and tape is described, and potential applications are outlined.

Tuesday, May 10

CHMT Luncheon Speaker
Mr. **Warren Fackler,** P.E., President, Telesis Systems, Inc.
"Opportunities for Intersociety Cooperation"

The rate of technological change is rapidly accelerating. Compounded with international economic competition, this rate of change imposes new demands on engineers who now must function in an increasingly multidisciplinary environment. Mr. Fackler explores how the members of the technological societies should respond to this challenge.

HYBRID MICROCIRCUITS

Chairman—**Brian T. Robertson,** *General Electric Ceramics, Inc.*
Assistant Chairman—**John R. Menaugh,** *E.I. duPont de Nemours & Co., Inc.*
Tom Berdner, *Lindberg*
David Thibault, *Engelhard Corporation*
Robert R. Sutherland, *British Telecom*
Warren L. Willis, *General Electric Company*
Courtland Robinson, *AT&T Bell Laboratories*
Joseph Soucy, *GTE Government Systems Corporation*
Patricia Kitano, *Boeing Aerospace*

INTERCONNECTIONS

Chairman—**Nick Panousis,** *IBM Corporation*
Assistant Chairman**Charles J. Speerschneider,** *Honeywell, Inc.*
Joe T. Dixon, *AT&T Bell Laboratories*
Peter M. Hall, *AT&T Bell Laboratories*
Jim Sim, *Allied Bendix Aerospace*
Les Fox, *Digital Equipment Corporation*
Harvey D. Solomon, *General Electric/CRD*
Dennis Olsen, *Motorola, Inc.*
Paul Totta, *IBM Corporation*

MANUFACTURING TECHNOLOGY

Chairman—**Steve Prough,** *Intel Corporation*
Assistant Chairman—**Alan Knight,** *IBM Corporation*
Michael Cassidy, *AT&T Technology Systems*
Bill Dalzell, *Polaroid Corporation*
John Fisher, *AT&T Engineering Research Center*
Archie Mones, *E.I. duPont de Nemours & Co., Inc.*
Ed Mayer, *AT&T Bell Laboratories*
Tony Supppelsa, *Motorola, Inc.*
Tom Poulin, *E.I. duPont de Nemours & Co., Inc.*

MATERIALS

Chairman—**C.G. Chen,** *Eaton Corporation*
Assistant Chairman—**Albert Lin,** *AT&T Bell Laboratories*
Assistant Chairman—**Hung C. Ling,** *AT&T Engineering Research Center*
D.M. Barnes, *AT&T Bell Laboratories*
Chris Needes, *E.I. duPont de Nemours & Co., Inc.*
John Lau, *Hewlett-Packard Company*
J.E. Billigmeier, *3M Company*
Frank Howland, *AT&T Bell Laboratories*
D.P. Seraphim, *IBM Corporation*

DISCRETE COMPONENTS

Chairman—**Jim Fresia,** *Sprague Electric Company*
Assistant Chairman—**James Murphy,** *AT&T Bell Laboratories*
Larry Burton, *Virginia Polytechnic Institute and State University*
Bill Carrier, *Mallory Capacitor Division/Emhart Corporation*
Barry Litner, *AT&T Technologies*
S.P. Sharma, *AT&T Bell Laboratories*
William Robbins, *Charles Stark Draper Laboratory*
Dennis Phalen, *Delco Electronics Corporation*
David G. Mould, *Northern Telecom Limited*
Gary J. Ewell, *Aerospace Corporation*
Pete Schneider, *AT&T Technology Systems*
Bob Spearman, *KEMET Electronics Corp.*
Albert F. Puttlitz, *IBM Corporation*

PACKAGING

Chairman—**Susan Schlough,** *AT&T Bell Laboratories*
Assistant Chairman—**John Stafford,** *Motorola, Inc.*
Jack Balde, *Interconnection Decision Consulting*
Ronald Kolc, *RCA Corporation*
Mali Mahalingam, *Motorola, Inc.*
Jon Prokop, *Cincinnati Microwave*
Paul VanLoan, *Hewlett-Packard Company*
Dick Landis, *Martin Marrietta*
W. Beckenbaugh, *Motorola, Inc.*
Steve Yingst, *AMP Incorporated*
Ron Potts, *IBM Corporation*
Camille Saheley, *Digital Equipment Corporation*
Ken Bishop, *General Electric Ceramics, Inc.*
John M. Segelken, *AT&T Bell Laboratories*
John Prince, *University of Arizona*

RELIABILITY

Chairman—**George G. Harman,** *National Bureau of Standards*
Assistant Chairman—**Melanie Iannuzzi-Glogovsky,** *AT&T Bell Laboratories*
David W. Bushmire, *Sandia National Laboratories*
Darvin Edwards, *Texas Instruments, Inc.*
James T. Lynch, *Plessey Research*
Patrick Thompson, *Gould Semiconductor Division*
Vern Winchell, *Motorola, Inc.*
Harry K. Charles, *The Johns Hopkins University*
Robert T. Howard, *IBM Corporation*
Ronald A. Thiel, *General Dynamics Electronics*

Contents

Session V
Connectors

Chairman: R.S. Mroczkowski, *AMP Incorporated*
Co-Chairman: B.T. Reagor, *Bell Communications Research*

Session VI
Fiber Optics

Chairman: G.J. Sellers, *Amphenol Products, Amphenol Products, Allied Signal, Inc.*
Co-Chairman: M.H. Weichold, *Texas A&M University*

Session VII
Multichip Packaging

Chairman: J. Segelken, *AT&T Bell Laboratories*
Co-Chairman: J. Balde, *Interconnection Decision Consulting*

Session VIII
Unique Manufacturing Process

Chairman: A.D. Knight, *IBM Corporation*

Co-Chairman: T. Poulin, *E.I. duPont de Nemours & Company, Inc.*

Session IX
Reliability/Discrete Components

Chairman: B. Spearman, *KEMET Electronics Corp.*

Co-Chairman: R. Thiel, *General Dynamics Electronics*

Session X
Advanced Packaging Technology

Chairman: R. Potts, *IBM Corporation*

Co-Chairman: J. Stafford, *Motorola, Inc.*

Session XI
Organic Materials

Chairman: D.M. Barnes, *AT&T Bell Laboratories*

Co-Chairman: J.E. Billigmeier, *3M Company*

Session XII
Reliability

Chairman: P. Thompson, *Gould Semiconductor Division*

Co-chairman: M. Iannuzzi-Glogovosky, *AT&T Bell Laboratories*

Session XIII
Interconnection Bonding

Chairman: J.T. Dixon, *AT&T Bell Laboratories*

Co-Chairman: D.R. Olsen, *Motorola, Inc.*

Session XIV
Inorganic Materials—Characterization and Processing

Chairman: A.W. Lin, *AT&T Bell Laboratories*

Co-chairman: F.L. Howland, *AT&T Bell Laboratories*

Session XV
Hybrid Technology

Chairman: *T. Berdner, Linberg*

Co-chairman: J. Soucy, *GTE Government Systems Corporation*

COULD COMPLIANT EXTERNAL LEADS REDUCE THE STRENGTH OF A SURFACE-MOUNTED DEVICE?

E. Suhir
AT & T Bell Laboratories
600 Mountain Avenue
Murray Hill, N.J. 07974

A simplified analytical model of hybrid-integrated-circuit (HIC)/printed-wire-board (PWB) assembly bowing is developed to explain a paradoxical situation, observed by T. F. Marinis, R. C. Reinert and W. M. Sherry during testing of compliant leaded HIC's: the bending moments applied to the PWB and caused the HIC fracture turned out in some tests smaller for greater lead compliance. We show that such a situation is due to the redistribution of the lead reactions at certain combinations of the HIC length, HIC and PWB fluxural rigidity, and lead spring constant. Our analysis indicates, that only sufficiently compliant leads could essentially reduce the stresses in the HIC, while leads of moderate compliance could result in even greater stresses than stiff leads. We suggest an easy-to-calculate governing parameter, which characterizes the mechanical behavior of HIC/PWB assemblies with compliant leads. The obtained results can be of help in physical design of compliant leaded surface mounted devices.

1. Introduction

T. F. Marinis, R. C. Reinert and W. M. Sherry [1] observed a paradoxical situation during testing of compliant leaded hybrid integrated circuits (HIC): in some tests the bending moment, applied to the printed wire board (PWB) and caused the HIC fracture, turned out smaller, when leads with greater compliance were installed. The authors indicated that they did not find an adequate explanation to this observation.

In this study we develop a simplified analytical model of HIC/PWB assembly bowing to find an explanation to the observed phenomenon. We treat the HIC and the PWB as elongated rectangular plates, connected by a continuous elastic attachment, and assume that the leads transmit the axial forces only. Therefore our model is not intended to be utilized for the prediction of the actual stresses in the assembly.

Note that various aspects of the performance and reliability of surface mounted devices with compliant leads were discussed in [1-6].

2. Theory

Basic Equation

Let a HIC/PWB assembly with compliant external leads be subjected to overall bending due to external moments $\mathcal{M}$ applied to the PWB (Fig. 1). We assume that the number of leads is sufficiently great and therefore these leads can be treated as a continuous elastic attachment.

We proceed from the following equations of the HIC and the PWB bowing:

$$D_1 w_1^{IV}(x) = q(x), \quad D_2 w_2^{IV}(x) = -\frac{b_1}{b_2} q(x), \tag{1}$$

where $w_1(x)$ and $w_2(x)$ are deflection functions for the HIC and the PWB,

$$D_1 = \frac{E_1 h_1^3}{12(1-\nu_1^2)}, \quad D_2 = \frac{E_2 h_2^3}{12(1-\nu_2^2)}$$

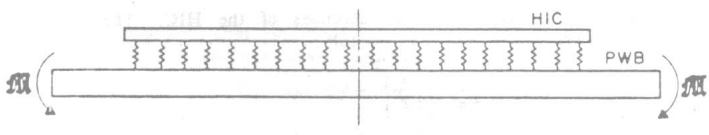

FIG. 1

are their fluxural rigidities; E_1, ν_1 and E_2, ν_2 are elastic constants of the HIC and the PWB materials, h_1 and h_2 are the HIC and the PWB thicknesses,

$$q(x) = k[w_2(x) - w_1(x)] \tag{2}$$

are the lead reaction forces per unit assembly length, k is the spring constant of the elastic attachment, and the ratio $\frac{b_1}{b_2}$ of the HIC and the PWB widths accounts for the effect of these widths on the HIC and the PWB rigidities. The origin is in the middle of the assembly.

The spring constant k of the elastic attachment is related to the spring constant K of a single lead by the formula:

$$k = \frac{mK}{2\ell b_1}, \tag{3}$$

where ℓ is the HIC half length, and m is the total number of leads (on both sides of the assembly).

After excluding the function q(x) from the equations (1) we obtain the following relationship between the fourth derivatives of the functions $w_1(x)$ and $w_2(x)$:

$$w_1^{IV}(x) + \eta w_2^{IV}(x) = 0, \tag{4}$$

where

$$\eta = \frac{b_2 D_2}{b_1 D_1} \tag{5}$$

is the PWB/HIC rigidity ratio. By integrating the equation (4) four times and using obvious boundary conditions

$$w_1''(\ell) = 0, \; w_1'''(\ell) = 0, \; w_2''(\ell) = \frac{\mathcal{M}}{b_2 D_2}, \; w_2'''(\ell) = 0, \; w_1'(0) = w_2'(0) = 0,$$

we obtain the relationship between the deflection functions $w_1(x)$ and $w_2(x)$ as follows:

$$w_1(x) + \eta w_2(x) = \frac{\mathcal{M}}{2 b_1 D_1} x^2. \tag{6}$$

Using (2) and (6) we rewrite the first of the equations (1) in the form:

$$w_1^{IV}(x) + 4\alpha^4 w(x) = \frac{2\alpha^4 \mathcal{M}}{(1+\eta) b_1 D_1} x^2, \tag{7}$$

where

$$\alpha = \sqrt[4]{\frac{K}{4 D_1}\left(1 + \frac{1}{\eta}\right)} = \sqrt[4]{\frac{Km(1+\eta)}{8 b_2 D_2 \ell}}. \tag{8}$$

The equation (7) is an equation of bending of a bar, lying on an elastic foundation and subjected to a distributed external load

$$p(x) = \frac{2\alpha^4 \mathcal{M}}{(1+\eta) b_1} x^2, \tag{9}$$

which is symmetric with respect to the middle of the bar. It is clear, that the solution to the equation (7) must also be symmetric with respect to the origin x = o, and, in addition, must satisfy the boundary conditions

$$w_1''(\ell) = 0, \; w_1'''(\ell) = 0. \tag{10}$$

0569-5503/88/0000-0001 $1.00 © IEEE

reflecting the fact, that no concentrated forces nor bending moments act at the end cross-sections of the HIC.

Solution to the Basic Equation

We present the solution to the equation (7) in the form:

$$w_1(x) = A_0 V_0(\alpha x) + A_1 V_1(\alpha x) + A_2 V_2(\alpha x) + A_3 V_3(\alpha x) + Cx^2, \quad (11)$$

where A_i, i = 0,1,2,3, are constants of integration, and Cx^2 is the particular solution to the equation (7). The functions $V_i(\alpha x)$, i = 0,1,2,3, are expressed as follows:

$$\left.\begin{aligned} V_0(\alpha x) &= \cosh\alpha x \cos\alpha x \\ V_1(\alpha x) &= \frac{1}{\sqrt{2}}(\cosh\alpha x \sin\alpha x + \sinh\alpha x \cos\alpha x) \\ V_2(\alpha x) &= \sinh\alpha x \sin\alpha x \\ V_3(\alpha x) &= \frac{1}{\sqrt{2}}(\cosh\alpha x \sin\alpha x - \sinh\alpha x \cos\alpha x) \end{aligned}\right\} \quad (12)$$

These functions have the following properties which make their utilization of convenience:

$$V_1'(\alpha x) = \alpha\sqrt{2}\, V_0(\alpha x), \quad V_2'(\alpha x) = \alpha\sqrt{2}\, V_1(\alpha x),$$

$$V_3'(\alpha x) = \alpha\sqrt{2}\, V_2(\alpha x), \quad V_0'(\alpha x) = -\alpha\sqrt{2}\, V_3(\alpha x), \quad (13)$$

$$V_0(0) = 1, \quad V_1(0) = V_2(0) = V_3(0) = 0. \quad (14)$$

After substituting the particular solution Cx^2 in the equation (7) we find:

$$C = \frac{\mathcal{M}}{2b_1 D_1 (1+\eta)}.$$

Since the solution (11) must be symmetric with respect to the origin x = 0, and the functions $V_1(\alpha x)$ and $V_3(\alpha x)$ are odd, then the constants A_1 and A_3 must be put equal to zero. Thus, the solution (11) yields:

$$w_1(x) = A_0 V_0(\alpha x) + A_2 V_2(\alpha x) + \frac{\mathcal{M}x^2}{2b_1 D_1 (1+\eta)}. \quad (15)$$

The constants A_0 and A_2 can be found on the basis of the boundary conditions (10). After substituting (15) into these conditions we obtain the following algebraic equations for the unknowns A_0 and A_2:

$$V_2(u)\, A_0 - V_0(u)\, A_2 = \frac{\mathcal{M}}{2\alpha^2 b_1 D_1 (1+\eta)},$$

$$V_1(u)\, A_0 + V_3(u)\, A_2 = 0, \quad (16)$$

where the parameter u of bending is given by the formula:

$$u = \alpha\ell = \sqrt[4]{\frac{Km(1+\eta)}{8b_2 D_2 \ell}}. \quad (17)$$

From (16) we find:

$$A_0 = \frac{\mathcal{M}\ell^2}{6b_1 D_1 (1+\eta)}\chi_1(u), \quad A_2 = -\frac{\mathcal{M}\ell^2}{2b_1 D_1 (1+\eta)}\frac{\phi_1(u)}{u^2}, \quad (18)$$

where the functions

$$\chi_1(u) = \frac{3}{u^2}\frac{V_3(u)}{V_0(u)V_1(u) + V_2(u)V_3(u)} =$$

$$= \frac{6}{u^2}\frac{\cosh u \sin u - \sinh u \cos u}{\sinh 2u + \sin 2u}, \quad (19)$$

$$\phi_1(u) = \frac{V_1(u)}{V_0(u)V_1(u) + V_2(u)V_3(u)} =$$

$$= 2\frac{\cosh u \sin u + \sinh u \cos u}{\sinh 2u + \sin 2u}, \quad (20)$$

are introduced in such a way, that they are equal to unity for an ideally compliant attachment (u = 0) and tend to zero for absolutely stiff leads ($u \to \infty$). The tabulated values of these functions are given in Table 1.

TABLE 1

u	$\phi_1(u)$	$\chi_1(u)$	$\chi_2(u)$	$\rho(u)$	x_*/ℓ
0	1.000	1.000	1.000	1.000	
0.1	1.000	1.000	1.000	1.000	
0.2	1.000	1.000	1.000	1.000	
0.3	0.999	0.999	0.999	0.999	
0.4	0.996	0.996	0.997	0.997	
0.5	0.990	0.991	0.993	0.993	
0.6	0.979	0.982	0.985	0.985	
0.7	0.961	0.967	0.973	0.973	
0.8	0.935	0.946	0.956	0.956	
0.9	0.899	0.917	0.931	0.931	
1.0	0.852	0.878	0.899	0.899	
1.1	0.795	0.830	0.859	0.859	
1.2	0.728	0.774	0.813	0.813	
1.3	0.653	0.712	0.761	0.761	
1.4	0.573	0.645	0.705	0.705	
1.5	0.492	0.576	0.648	0.618	
1.6	0.411	0.509	0.591	0.591	
1.7	0.335	0.444	0.537	0.537	
1.8	0.264	0.384	0.483	0.483	
1.9	0.201	0.328	0.439	0.439	
2.0	0.144	0.279	0.397	0.387	
2.2	0.054	0.197	0.325	0.325	
2.37	0.000	0.147	0.279	0.410	0
2.4	-0.009	0.136	0.269	0.392	0.137
2.6	-0.051	0.092	0.226	0.352	0.330
2.8	-0.074	0.060	0.193	0.327	0.400
3.0	-0.085	0.038	0.167	0.302	0.470
3.2	-0.087	0.023	0.146	0.300	0.500
3.4	-0.082	0.012	0.129	0.29[illegible]	0.530
3.6	-0.073	0.006	0.115	0.303	0.507
3.8	-0.063	0.002	0.104	0.312	0.509
4.0	-0.052	-0.001	0.094	0.322	0.607
4.2	-0.041	-0.002	0.085	0.320	0.626
4.4	-0.031	-0.003	0.078	0.318	0.643
4.6	-0.022	-0.003	0.071	0.315	0.658
4.8	-0.015	-0.002	0.065	0.313	0.673
5.0	-0.009	-0.002	0.060	0.311	0.686

After substituting the formulas (18) for the constants of integration in (15) we obtain the solution to the basic equation (7) as follows:

$$w_1(x) = \frac{\mathcal{M}\ell^2}{2b_1 D_1 (1+\eta)}\left[\left[\frac{x}{\ell}\right]^2 + \frac{\chi_1(u)}{3}V_0(\alpha x) - \frac{\phi_1(u)}{u^2}V_2(\alpha x)\right] \quad (21)$$

Deflections

The equation (21) determines the deflections of the HIC. The deflections of the PWB can be obtained from (6):

$$w_2(x) = \frac{\mathcal{M}\ell^2}{2b_1 D_1 (1+\eta)}\left[\left[\frac{x}{\ell}\right]^2 - \right.$$

$$\left. - \frac{1}{\eta}\left[\frac{\chi_1(u)}{3}V_0(\alpha x) - \frac{\phi_1(u)}{u^2}V_2(\alpha x)\right]\right]. \quad (22)$$

The bows of the HIC and the PWB in the middle of the assembly can be determined by the formulas:

$$f_1(0) = w_1(\ell) - w_1(0) = \frac{\mathcal{M}\ell^2}{6b_1D_1(1+\eta)}\left[3-\chi_1(u)-2\chi_2(u)\right]$$

$$f_2(0) = w_2(\ell) - w_2(0) = \frac{\mathcal{M}\ell^2}{6b_1D_1(1+\eta)}\left[3+\frac{1}{\eta}\left(\chi_1(u)+2\chi_2(u)\right)\right] \quad (23)$$

where the function

$$\chi_2(u) = \frac{\chi_1(u)}{3}\left[V_0(u)-1\right] - \frac{\phi_1(u)}{u^2}V_2(u) =$$

$$= \frac{3}{u^2}\,\frac{V_1(u)V_2(u)-V_0(u)V_3(u)}{V_0(u)V_1(u)+V_2(u)V_3(u)} = \frac{3}{2u^2}\,\frac{\sinh 2u-\sin 2u}{\sinh 2u+\sin 2u} \quad (24)$$

is also equal to unity when u is zero and tends to zero for $u \to \infty$. The tabulated values of this function are given in Table 1. Obviously, for ideally compliant leads ($u=0$) the HIC bow $f_1(0)$ is zero, and the PWB bow $f_2(0)$ is the maximum and is expressed by the formula:

$$f_2(0) = \frac{\mathcal{M}\ell^2}{2b_2D_2}.$$

For absolutely stiff leads ($u \to \infty$) we have:

$$f_1(0) = f_2(0) = \frac{\mathcal{M}\ell^2}{2b_1D_1(1+\eta)}.$$

Evidently, the formulas (23) determine the maximum values of the HIC and the PWB bows, as long as the deflection functions $w_1(x)$ and $w_2(x)$ do not have more than one internal extremum in the mid-cross-section. In order to find out whether these functions could have more than one internal extremum, we proceed from the fact, that when the extremum at $x = 0$ is the only one, it is the absolute minimum. In this case the curvature at this cross-section is positive. However, if there is more than one extremum in the deflection function within the assembly length, the extremum at $x = 0$ is just the local maximum (Fig. 2), while it is the "additional" extrema, which represent the absolute minima of the deflection function. In this case the curvature at $x = 0$ must be negative.

The equations (21) and (22) result in the following formulas for the HIC and the PWB curvatures:

$$w_1''(x) = \frac{\mathcal{M}}{b_1D_1(1+\eta)}\left[1-\frac{u^2\chi_1(u)}{3}V_2(\alpha x)-\phi_1(u)V_0(\alpha x)\right]$$

$$w_2''(x) = \frac{\mathcal{M}}{b_1D_1(1+\eta)}\left[1+\frac{1}{\eta}\left(\frac{u^2\chi_1(u)}{3}V_2(\alpha x)+\phi_1(u)V_0(\alpha x)\right)\right] \quad (25)$$

The curvatures at $x = 0$ are as follows:

$$w_1''(0) = \frac{\mathcal{M}_0}{b_1D_1(1+\eta)}\left[1-\phi_1(u)\right], \quad (26)$$

$$w_2''(0) = \frac{\mathcal{M}_0}{b_1D_1(1+\eta)}\left[1+\frac{1}{\eta}\phi_1(u)\right]. \quad (27)$$

Since the function $\phi_1(u)$ never exceeds unity (see Table 1), the curvature $w_1''(0)$ is always positive. Therefore the deflection function $w_1(x)$ for the HIC has always a minimum at $x = 0$. No additional extrema are possible. Therefore, the $f_1(0)$ value always represents the maximum bow of the HIC. In the case of the PWB, however, the $f_2(0)$ value determines the maximum bow only if the inequality

$$1+\frac{1}{\eta}\phi_1(u) > 0$$

takes place. Hence,

$$1-\phi_1(u) > 1+\eta \quad (28)$$

is the condition, that additional extrema occur on the PWB deflection curve. The function $1-\phi_1(u)$ is plotted in Fig. 3.

Obviously, in order that the inequality (28) could take place, the function $\phi_1(u)$ must be negative (this is a necessary, though, of course, an insufficient condition of the additional extrema). To determine the u values, for which the function $\phi_1(u)$ is negative, we use the formula (20). As one could see from the Fig. 3, the maxima of the function $1-\phi_1(u)$ occur in the region of rather great u values ($u > 2$). Therefore the

FIG. 2

negative values of the function $\phi_1(u)$ also occur in this region. For sufficiently great u values the formula (20) can be simplified as follows:

$$\phi_1(u) \cong 2e^{-u}(\sin u + \cos u). \quad (29)$$

Hence,

$$\phi_1'(u) = -4e^{-u}\sin u, \quad (30)$$

$$\phi_1''(u) = 4e^{-u}(\sin u - \cos u). \quad (31)$$

As evident from (30), the extrema of the function $\phi_1(u)$ take place for

$$u = m\pi, \quad m = 0,1,2,... \quad (32)$$

Substituting (32) in (31) we obtain:

$$\phi_1''(m\pi) = -4e^{-m\pi}\cos m\pi, \quad m = 0,1,2,...$$

The extrema of the function $\phi_1(u)$ are minima, when the $\phi_1''(m\pi)$ values are positive. This occurs for odd m numbers. Hence, the minima of the function $\phi_1(u)$ are as follows:

$$\phi_{1,\min} = -2e^{-m\pi}, \quad m = 1,3,5,...$$

Therefore the maxima of the function $1-\phi_1(u)$ are

$$\left(1-\phi_1\right)_{\max} = 1+2e^{-m\pi}, \quad m = 1,3,5,...$$

This formula indicates, that only the first maximum $(1-\phi_1)_{\max} = 1.0864$ is essentially different from unity. Therefore, from the practical standpoint, the additional extrema on the PWB deflection function $w_2(x)$ can occur only for those u values, where the first maximum of the function $1-\phi_1(u)$ takes place. These values are located between the first two zeros of the function $\phi_1(u)$. Using (29), we conclude that the zeros of the function $\phi_1(u)$ occur for the u values which could be found from the equation $\tan u = -1$, i.e. for

$$u_m = -\frac{\pi}{4} + m\pi, \quad m = 1,2,...$$

The first two roots of this equation are:

$$u_1 = \frac{3}{4}\pi = 2.3562, \quad u_2 = \frac{7}{4}\pi = 5.4978. \quad (33)$$

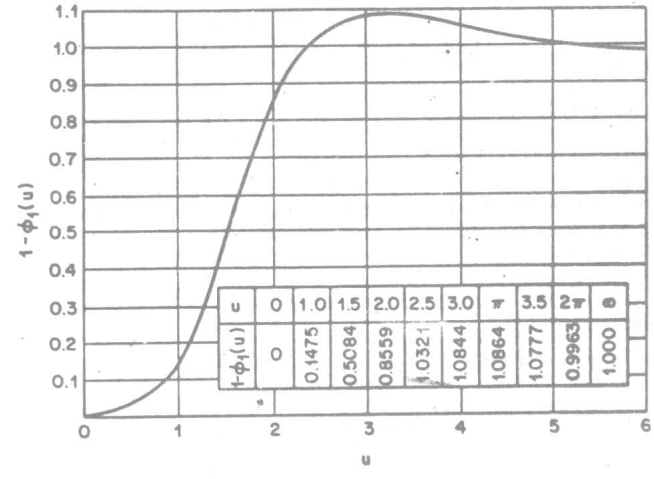

u	0	1.0	1.5	2.0	2.5	3.0	π	3.5	2π	∞
1-φ1(u)	0	0.1475	0.5084	0.8559	1.0321	1.0844	1.0864	1.0777	0.9963	1.000

FIG. 3

Thus, in order to determine whether additional extrema on the PWB deflection function could occur, one should calculate the u value by the formula (17), and, if this value falls into the range between the u_1 and u_2, to check, if the stronger condition (28) is fulfilled. Evidently, if the η value is greater than 0.0864, no additional extrema could occur at all, whatever the u value. Therefore, the lead compliance can affect the shape of the PWB deflection function only for very flexible PWB's.

Bending Moments

The bending moments acting over the HIC and the PWB cross-sections can be easily obtained from the formulas (25) for the curvatures:

$$\left.\begin{aligned} M_1(x) &= M_\infty \left[1 - \frac{u^2\chi_1(u)}{3} V_2(\alpha x) - \phi_1(u)\, V_0(\alpha x)\right] \\ M_2(x) &= \left[\eta + \frac{u^2\chi_1(u)}{3} V_2(\alpha x) + \phi_1(u)\, V_0(\alpha x)\right] \end{aligned}\right\}, \quad (34)$$

where

$$M_\infty = \frac{\mathcal{M}}{1+\eta} \quad (35)$$

is the bending moment for the stiff leaded HIC. Obviously, the sum $M_1(x)$ and $M_2(x)$ is always constant and is equal to the external moment $\mathcal{M}$.

The maximum bending moment in the PWB occurs at $x \geqslant \ell$ and is equal to $\mathcal{M}$. As far as the HIC is concerned, the maximum bending moment always acts in its mid-cross-section $x = 0$ and is expressed by the formula:

$$M_1(0) = M_\infty \left[1 - \phi_1(u)\right], \quad (36)$$

where the function $1 - \phi_1(u)$ reflects the effect of the lead compliance. This function was analyzed in the previous section.

As has been shown, the maximum value of the function $1 - \phi_1(u)$ is equal to 1.0864. When the combination of the factors, affecting the mechanical behavior of the HIC/PWB assembly, results in a u value within the range between the $u_1 \cong 2.36$ and $u_2 \cong 5.50$, then the maximum bending moment in the HIC becomes greater than the bending moment M_∞. Hence, the application of compliant leads (or, more precisely, the application of leads with an inappropriately chosen spring constant) adversely affects the HIC strength in this case. When the parameter u is within the range between π, (where the bending moment (36) is maximum), and $u_2 \cong 5.5$ value, then, as evident from Fig. 3, the increase in the lead compliance (decrease in the u value) results in greater, but not smaller, bending moments in the HIC. This paradoxical situation was experimentally detected by the authors of the reference [1]. The u values calculated for the tested HIC/PWB assemblies when this situation took place, are somewhat greater than π.

Fig. 3 shows also, that in order to achieve essential reduction in the HIC bending moment, the compliance of the employed leads must be sufficiently great, and the value of the parameter u be smaller than $u_1 \cong 2.36$. If the spring constant of the chosen compliant lead design results in the u values exceeding $u_2 \cong 5.50$, then the strength of the compliant leaded HIC structure will not be different from the strength of the HIC with absolutely stiff leads. Note, that in the tests, described in the reference [1], the calculated u values for the HIC/PWB assemblies are $u \cong 3.2$ for the BMPM type of the PWB with "rigid" NAS leads ($K = 1000$ lb/in) and $u \cong 2.7$ for "compliant" mod 1 leads ($K = 500$ lb/in). Finally, if the u value falls within the range between the $u_1 \cong 2.36$ and $u_2 \cong 5.5$, then the compliant leads result in even greater bending moments in the HIC, than absolutely stiff leads. The adverse effect of the lead compliance in such a situation cannot exceed, however, 8.6%.

Lead Reactions

The shearing forces acting over the HIC and the PWB cross-sections can be found from the formulas (34) by differentiation:

$$N(x) = \frac{dM_1(x)}{dx} = -\frac{dM_2(x)}{dx} =$$

$$= \sqrt{2}\, M_\infty \frac{u}{\ell}\left[\frac{u^2\chi_1(u)}{3} V_1(\alpha x) - \phi_1(u)\, V_3(\alpha x)\right]. \quad (37)$$

Obviously, $N(0) = N(\ell) = 0$.

The lead reactives can be found either by substituting the formulas (21) and (22) in (2), or by differentiating the equation (37):

$$q(x) = 2M_\infty \left(\frac{u}{\ell}\right)^2 \left[\frac{u^2\chi_1(u)}{3} V_0(\alpha x) - \phi_1(u)\, V_2(\alpha x)\right]. \quad (38)$$

The reactions in the middle ($x = 0$) and at the ends ($x = \ell$) of the assembly are as follows:

$$q(0) = M_\infty \left(\frac{2u}{\ell}\right)^2 \frac{\chi_1(u)}{6}, \quad q(\ell) = -M_\infty \left(\frac{2u}{\ell}\right)^2 \frac{\chi_2(u)}{3}, \quad (39)$$

where the function $\chi_2(u)$ is determined by (24). For sufficiently great u values (say, $u > 2$) the functions $\chi_1(u)$ and $\chi_2(u)$ can be evaluated by the formulas

$$\chi_1(u) = \frac{6}{u^2} e^{-u}(\sin u - \cos u), \quad \chi_2(u) = \frac{3}{2u^2}. \quad (40)$$

Then the formulas (39) yield:

$$q(0) \cong 4\, \frac{M_\infty}{\ell^2} e^{-u}(\sin u - \cos u), \quad q(\ell) \cong -2\, \frac{M_\infty}{\ell^2}. \quad (41)$$

Thus, when the leads are stiff (great u values), the lead reactions in the middle of the assembly rapidly decrease with an increase in the lead stiffness, while the end reactions remain more or less constant.

In order to find out whether the function (38) has extrema, additional to (39), we use the following formula for the "curvature"

$$q''(0) = -M_\infty \left(\frac{2u^2}{\ell^2}\right)^2 \phi_1(u).$$

For $u < 2.36$ the function $\phi_1(u)$ is positive, then the "curvature" $q''(0)$ is negative, and therefore the first of the formulas (39) represents the maximum of the reaction force function. No other internal extrema occur in this case. For greater u values, however, when the function $\phi_1(u)$ is negative, the "curvature" $q''(0)$ becomes positive, and the first of the formulas (39) determines a local minimum.

The maxima of the reaction force function, when the u value is greater than 2.36, occur at the locations $x = x_*$, which can be found from the equation $q'(x)|_{x=x_*} = 0$. After substituting (38) into this equation we obtain the following transcendental equation for the x_* value:

$$\frac{u^2\chi_1(u)}{3} V_3\left(u\,\frac{x_*}{\ell}\right) + \phi_1(u)\, V_1\left(u\,\frac{x_*}{\ell}\right) = 0.$$

Using formulas (12), (19) and (20), we rewrite this equation as follows:

$$\tanh u \tanh\left(u\,\frac{x_*}{\ell}\right) + \tan u \tan\left(u\,\frac{x_*}{\ell}\right) = 0. \quad (42)$$

The numerical solution to this equation is plotted in Fig. 4.

For sufficiently great u values (say, $u > 3$) the equation (42) could be simplified:

$$\tan u \tan\left(u\,\frac{x_*}{\ell}\right) = -1.$$

The smallest root of this equation is

$$\frac{x_*}{\ell} = 1 - \frac{\pi}{2u}. \quad (43)$$

This formula and the Fig. 4 indicate that the maxima of the reaction forces shift towards the assembly ends with an increase in the lead stiffness (greater u values). These maxima can be calculated on the basis of the formula (38) and are as follows:

$$q(x_*) = M_\infty \left(\frac{2u}{\ell}\right)^2 \frac{\rho(u)}{3}, \quad (44)$$

where the tabulated values of the function

$$\rho(u) = \frac{3}{2}\left[\frac{u^2\chi_1(u)}{3} V_0\left(u\,\frac{x_*}{\ell}\right) - \phi_1(u)\, V_2\left(u\,\frac{x_*}{\ell}\right)\right] \quad (45)$$

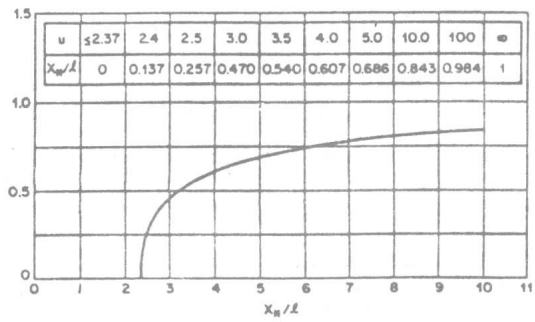

FIG. 4

are given in Table 1. For sufficiently great u $\frac{x_*}{\ell}$ values the formulas (12) for the $V_0\left(u\frac{x_*}{\ell}\right)$ and $V_2\left(u\frac{x_*}{\ell}\right)$ values can be simplified:

$$V_0(\alpha x_*) = \frac{1}{2}e^{u-\frac{\pi}{2}}\sin u, \quad V_2(\alpha x_*) = -\frac{1}{2}e^{u-\frac{\pi}{2}}\cos u .$$

Substituting these formulas and the formulas (29) and (40) in (45), we obtain: $\rho(u) = \frac{3}{2}e^{-\pi/2} = 0.3118$. Then the formula (44) yields:

$$q(x_*) = 2e^{-\frac{\pi}{2}} M_\infty \left(\frac{u}{\ell}\right)^2 \cong 0.4158\, M_\infty \left(\frac{u}{\ell}\right)^2 . \qquad (46)$$

This formula indicates, that when the lead stiffness is great (great u values), the maxima of the reaction force function rapidly increase with an increase in the u value (Fig. 5).

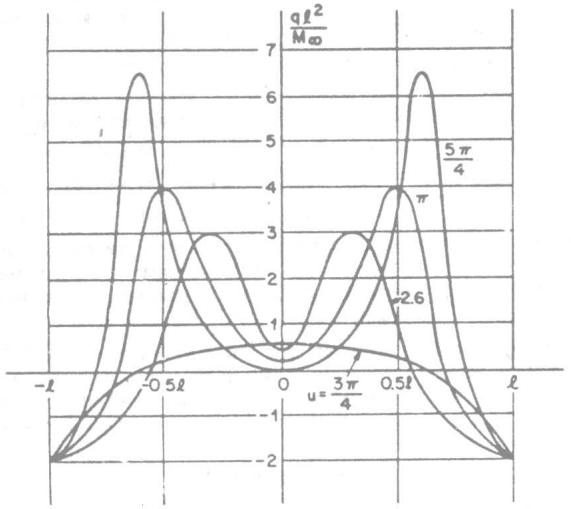

FIG. 5

3. Numerical Example

The numerical example is executed for an HIC (ℓ = 1in, b_1 = 1.2in, h_1 = 0.027in, $E_1 = 53.0 \times 10^6$ psi) attached to a PWB (b_2 = 2.5in, h_2 = 0.062in, $E_2 = 2.45 \times 10^6$ psi) by means of m = 40 compliant leads. We assume that the lead stand-off is small and may not be considered. The ultimate normal stress for the HIC material is σ_u = 30000 psi. The bending moment in the HIC which results in the ultimate stress σ_u is $M_1(0) = \frac{1}{6} b_1 h_1^2 \sigma_u$. The corresponding external moment applied to the PWB is

$$\mathcal{M} = \frac{1+\eta}{6} \cdot \frac{\sigma_u h_1^2}{1-\phi_1(u)} . \qquad (47)$$

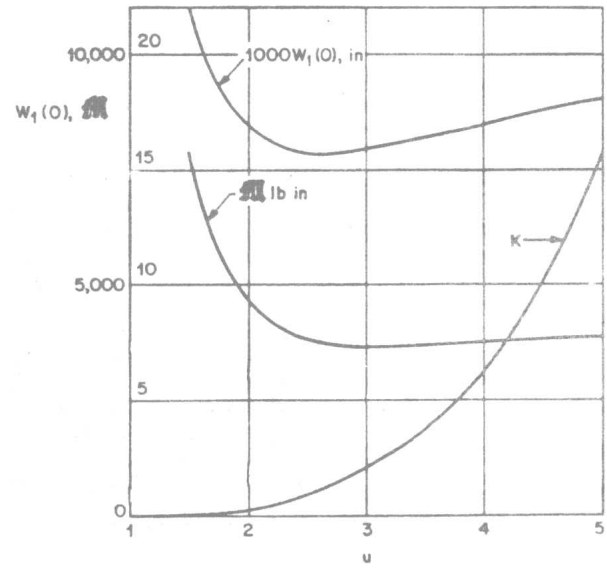

FIG. 6

TABLE 2

u	1.5	2.0	2.6	2.8	3.0	4.0	5.0	10.0
K, lb/in	64	203	579	779	1027	3244	7921	126735
$\mathcal{M}$ lb/in	15.539	9.222	7.511	7.350	7.276	7.504	7.824	7.893
$\phi_1(u)$	0.492	0.144	-0.051	-0.074	-0.085	-0.052	-0.009	-1.256×10
$\chi_1(u)$	0.576	0.279	0.092	0.060	0.038	-0.001	-0.002	8.0358×10
$\chi_2(u)$	0.648	0.397	0.226	0.193	0.167	0.094	0.060	0.03
$w_1(0)$, in	0.0217	0.0169	0.0158	0.0159	0.0160	0.0172	0.0181	0.0186
$q(\ell)$, psi	13.95	9.016	7.065	6.847	6.733	6.948	7.226	14.578

The calculations are carried out for different spring constant values, which, for the given u values, were evaluated by using the formula (17). The ultimate external moments were calculated by the formula (47). The calculated data is shown in Table 2 and plotted in Fig. 6. The distribution of the lead reactions, shearing forces, bending moments and deflections along the HIC/PWB assembly is shown in Table 3 and plotted in Fig. 7 for the case u = 2.8.

4. Discussion

Our analysis has indicated that the mechanical behavior of the compliant external leads in HIC/PWB assemblies can be characterized by the parameter u, which is defined by the formula (17). This governing parameter reflects the combined effect of HIC and PWB fluxural rigidities, HIC length, and the stiffness of the external leads. The mechanical behavior of the assembly and, in particular, the effect of the compliant leads is different for different u value ranges.

When the u value is small (compliant leads, short and rigid HIC, rigid PWB), the bending moment in the HIC mid-cross-section increases with an increase in the u value, and the self-equilibrated lead reactions are distributed in such a way, that their maximum (positive) values occur in the middle of the assembly, and the minimum (negative) values take place at the HIC ends. This situation remains, until the parameter u reaches the value $u = \frac{3\pi}{4} = 2.3562$, which corresponds to the situation, when the bending moment in the HIC mid-cross-section becomes equal to the bending moment M_∞ [illegible] leads. Then two new extrema

TABLE 3

$\frac{x}{\ell}$	0	0.2	0.4	0.6	0.8	0.9	1.0
q(x), psi	8.344	9.441	11.017	7.612	-10.245	-28.269	-54.078
N(x), lb×in	0	1.746	3.816	5.830	5.904	4.039	0
$M_1(x)$, lb×in	-3.645	-3.474	-2.923	-1.948	-0.716	-0.204	0
$M_2(x)$, lb×in	-3.705	-3.876	-4.427	-5.402	-6.634	-7.146	-7.350
$w_1(x) \times 10^3$, in	0	0.740	2.888	6.216	10.333	12.533	14.757
$w_2(x) \times 10^3$, in	0	0.655	2.681	6.272	11.767	15.360	19.577

(maxima) begin to form on the lead reaction function ("flanking" the x = 0 cross-section). The middle and the end reactions start to decrease, while the "new" maxima rapidly increase. With the further increase in the u value, these maxima shift towards the assembly ends. Such a redistribution of the reaction forces results in the fact, that the bending moment in the PWB mid-cross-section becomes smaller, compared to the case of absolutely stiff leads, while the bending moment in the HIC exceeds the M_∞ value. The bending moment in the HIC reaches its maximum value $M_1(0) = 1.0864\ M_\infty$ when the parameter u is equal to π. In this situation the maxima of the lead reaction function are about twice as great as the negative end reactions, while the lead reaction in the middle of the assembly is only about 4% of the maximum reactions. The further

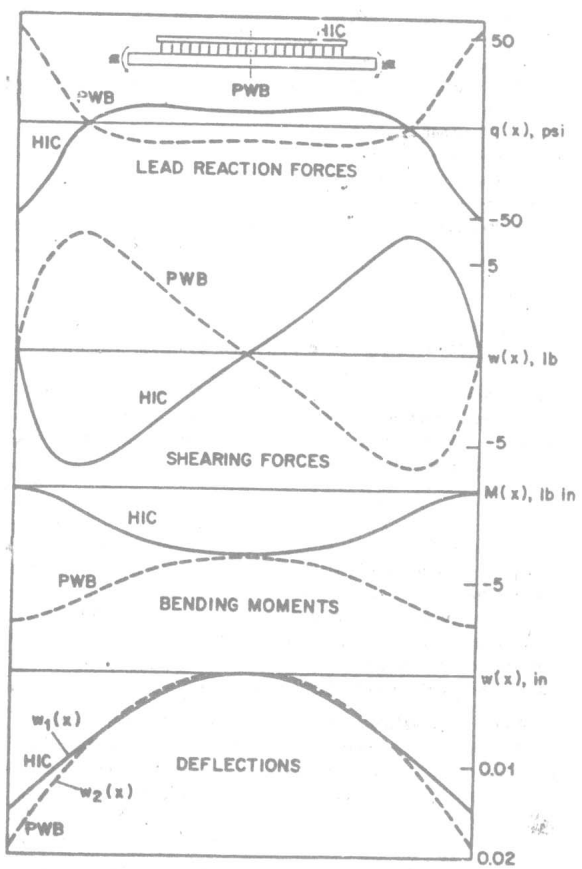

FIG. 7

growth of the parameter u (lead stiffness) results in smaller bending moments in the HIC. This is due to the fact that the lead reactions in the cross-sections in the vicinity of the middle of the assembly rapidly decrease, while the end reactions remain practically unchanged. At the same time, the growth in the maximum reactions is not yet sufficient to outweigh the favorable effect of the decrease in the reactions in the middle part of the assembly. Such a situation continues till $u = \frac{7\pi}{4} = 5.498$, when the bending moment HIC reaches the M_∞ value again. After that it does not practically change with the further increase in the u value (lead stiffness). When the u value is great, the reaction forces in the inner part of the assembly are very small, the end reactions are equal to the values they reached at $u = \pi$, (when the bending moment in HIC was maximum), and the maxima of the reation forces are very great. These maxima are located in the vicinity of the assembly ends.

Thus, in order to achieve substantial reduction in the HIC bending moment due to the application of compliant leads, the governing parameter u has to be smaller than $\frac{3\pi}{4}$. For $u > 5.5$ the change in the lead compliance does not practically affect the bending moment in the HIC. This fact could be used as a guidance to evaluate the feasibility of the leads with the given compliance, or for choosing an appropriate lead design for the given HIC/PWB assembly.

5. *Conclusions*

The following major conclusions can be drawn from the above analysis.

- An experimentally observed paradoxical situation, when the ultimate bending moments turned out in some cases smaller for leads of greater compliance, is due to the redistribution of lead reactions at certain combinations of the assembly length, HIC and PWB flexural rigidities and lead compliance. Our analysis indicated that only sufficiently compliant leads can essentially reduce the stresses in the HIC and the lead reactions, while leads of moderate compliance could result in even greater stresses in the HIC, than absolutely stiff leads. The adverse effect of the compliant leads in such a situation cannot exceed, however, 8.6%.

- We suggest an easy-to-calculate governing parameter, which characterizes the mechanical behavior of surface mounted devices with compliant leads. When this parameter is smaller than $\frac{3\pi}{4}$, the application of compliant leads results in smaller stresses. When this parameter is greater than $\frac{7\pi}{4}$, the "compliant" leads do not practically affect the mechanical behavior of the assembly compared to the case of absolutely stiff leads. If the calculated values of the parameter u fall into the range between the above values, the application of compliant leads has an adverse effect on the HIC strength.

- The obtained results can be of help in physical design of HIC/PWB and similar assemblies with compliant leads. They could be used as a guidance for a preliminary evaluation of the feasibility of the given compliant leads, or for choosing an appropriate compliant lead design for the given assembly.

Acknowledgment

The author is thankful to J. M. Segelken, C. J. Bartlett and P. M. Hall for useful comments.

References

1. Marinis, T. F., Reinert, R. C., Sherry, W. M., Impact of external lead design on the fracture of HIC-PWB assemblies subjected to bending, Proc. of the 34-th ECC, May 14-16, 1984, New Orleans, Louisiana.
2. Blade, J. W., Problems in the shift to leaded chip carrier construction - An overview, 4-th Annual IEPS Proceedings, October 1984.
3. Engelmaier, W., Test method considerations for SMT soldered joint reliability, Ibid.
4. Landis, R. C., J - leads for chip carriers: a comparative evaluation, Ibid.
5. Engelmaier, W., IEEE Compliant Lead Task Force-Phase I, 5-th Annual IEPC Proceedings, October 21-23, 1985, Orlando, Florida.
6. Kotlowitz, R. W. and Engelmaier, W., Impact of lead compliance on the solder attachment reliability of leaded surface mounted devices, 6-th Annual IEPC Proceedings, November 17-19, 1986, San-Diego, California.

THE INFLUENCE OF HOLD TIME AND FATIGUE CYCLE WAVE SHAPE ON THE-LOW CYCLE FATIGUE OF 60/40 SOLDER

Harvey D. Solomon

General Electric Corporate Research and Development Center
P.O. Box 8, K-1 / 3A51
Schenectady, N.Y. 12301

ABSTRACT

Previous experiments have shown that the fatigue life, N_f, is reduced when the cycling frequency, ν, is reduced. These tests utilized simple, symetric ramp loading with equal loading and unloading rates. While this sort of cycling is useful in identifying the influence of cycling frequency, it does not reproduce the type of loading actual solder joints experience. Actual duty cycles generally consist of a relatively rapid change in temperature, then a relatively long hold at a more or less constant temperature, followed by a relatively rapid temperature change back to the starting point and another hold time. To investigate this sort of cycling, isothermal experiments were performed with varying hold times rather than by varying the ramp loading and unloading rates. Failure was induced by the application of mechanical strains, at a constant temperature, rather than by the application of thermal strains. It was found that the frequency dependence of the fatigue life, induced by varying the hold time, was similar to that observed when the frequency was varied by changing the ramp loading and unloading rates. The frequency effect is actually somewhat less for the hold time tests than for the ramp loading tests. This difference is due to the load relaxation which takes place during the hold times. This relaxation is described and relaxation rate curves are provided.

Another feature of actual duty cycles is a significant asymetry in the cyclic load which develops due to the lower flow stress at temperatures above 50°C and the much higher flow stress developed below 0°C. The influence of this asymetry was examined by using differing loading and unloading rates. The flow stress is highly rate dependent, so utilizing a low loading rate requires a lower flow stress than if a higher loading rate was utilized. Using a low loading rate is thus equivalent to using a much higher temperature. The load asymetry has a significant influence on the fatigue life. Above about 3×10^{-4} to 3×10^{-3} Hz (depending upon the temperature), asymetric loading reduces the fatigue life by a factor of about 3. At lower frequencies, however, the lives for symetric and asymetric cycles are the same. Possible reasons for this are discussed.

Introduction

Fatigue in service applications results from a complex loading cycle, generally involving hold times and asymetric (unequal loading and unloading rates) cycles. These are the types of loading considered in this study, which is an outgowth of previous studies[1-4] conducted on 60/40 solder joints, where the fatigue life was determined from experiments utilizing symetric, fully reversed ramp loading with no hold time. In these previous tests, the same total shear strain rate was utilized for loading and unloading, to the same absolute value of plastic strain (i.e., from $+ \gamma_p$ to $- \gamma_p$ at the same rate). The influence of cycle frequency was studied by varying the strain rate while keeping the plastic strain limits constant[2,3]. These studies showed that below 10^{-3} Hz, the fatigue life was reduced by lowering the frequency. Above 10^{-3} Hz, there was little or no frequency influence on the fatigue. It was found[2-3] that the data could be described by a time modified strain range partitioning approach with the low frequency data described by a constant time to failure.

In the study described here, two different types of fatigue cycles were studied. In one set of experiments, the test specimen was strained at a relatively rapid rate (roughly 2 seconds to go from one plastic strain limit to the other), and then the total strain was held constant for a hold time. After this hold time period, the direction of straining was reversed until the other plastic strain limit was reached, whereupon the total strain was held constant for the same hold time period. The hold time and plastic strain limits were kept constant while the length of the hold time period was varied from test to test.

In the second set of experiments, the rate of straining and the rate of straining in the opposite direction were unequal, with no hold time between the two. The positive total strain rate (i.e., the strain rate from the negative plastic strain limit to the positive limit) was varied from test to test while the negative strain rate was kept constant. Low strain rates were characterized by more creep, thus to use the parlance of strain range partitioning, these were $\Delta\gamma_{pc}$ experiments[5]. This paper will contrast the results previously obtained with symetric ramp loading

0569-5503/88/0000-0007 $1.00 © IEEE